Transactions of the Korean Nuclear Society Autumn Meeting
Gyeongju, Korea, October 27-28, 2016

Monte Carlo analysis of megavoltage x-ray interaction-induced signal and noise in detectors for container inspection

Jinwoo Kim[a], Jiwoong Park[a], Junwoo Kim[a], Dong Woon Kim[a],
Chang Hwy Lim[b] and Ho Kyung Kim[a,c*]
[a]*School of Mechanical Engineering, Pusan National University, Busan 46241, South Korea*
[b]*Ocean System Engineering Division, Korea Research Institute of Ships & Ocean Engineering, Daejeon 34103, South Korea*
[c]*Center for Advanced Medical Engineering, Pusan National University, Busan 46241, South Korea*
[*]*Corresponding author: hokyung@pusan.ac.kr*

1. Introduction

Related to homeland security and contraband control, megavoltage (MV) x-ray scanning system may increase the effectiveness and efficiency of cargo screening at the port.

In a scanner system, a scintillation crystal is the first stage in the cascaded imaging chain transferring x-ray interaction information in cargo to be investigated to the final user who investigates x-ray images. On the other hand, the signal and noise is irreversibly transferred through the cascaded imaging chain. Therefore, the imaging performance of the first stage scintillator mainly governs the ultimate imaging performance of the system.

In MV imaging, it is generally accepted that high-density scintillators,[1] because of their sufficient optical yield, and low optical self-absorption and scattering coefficients. We chose the $CdWO_4$ as the scintillation material. $CdWO_4$ has a high density (7.9 g/cm^3), high atomic number (64), resistance to radiation,[2,3] high optical yield,[4] and low optical self-absorption.[4]

The purpose of this study is to quantify the MV x-ray interaction-induced signal-to-noise performance of the single block of $CdWO_4$ in terms of detective quantum efficiency (DQE), which provides the best signal-to-noise efficiency that we can achieve in the x-ray scanning system.

2. Methods

2.1 Moment analysis of AED

For an incident x-ray spectrum $S(E)$ with $\int_0^\infty S(E)d\mathrm{E} = 1$, the absorbed energy distribution (AED) recorded in a detector can be given by Eq. (1).

$$A(E) = \int_0^\infty E^n \cdot A(E, E')d\mathrm{E}' \quad (1)$$

where $A(E,E')$ is the detector response function describing the probability of depositing energy E given an incident photon with energy E'.

Then, the n-th moment of AED is given by Eq. (2).

$$M_n = \int_0^\infty E^n \cdot A(E)d\mathrm{E} \quad (2)$$

thus, the 0th moment of AED, that is quantum efficiency (QE), is given by Eq. (3).

$$M_0 = \int_0^\infty A(E)d\mathrm{E} \quad (3)$$

and the first and second moments of AED are given by Eqs. (4) and (5).

$$M_1 = \int_0^\infty E \cdot A(E)d\mathrm{E} \quad (4)$$

$$M_2 = \int_0^\infty E^2 \cdot A(E)d\mathrm{E} \quad (5)$$

then, the Swank noise factor and the DQE can be given by Eqs. (6) and (7).

$$\mathrm{I} = \frac{M_1^2}{M_0 \cdot M_2} \quad (6)$$

$$\mathrm{DQE} = \alpha \cdot I = \frac{M_1^2}{M_2} \quad (7)$$

2.2 Monte Carlo simulations

For a linear scintillation crystal and photodiode array, as shown in Fig. 1, MC simulations using Monte Carlo N-Particle transport code (MCNP version 5, RSICC, Oak Ridge, TN, USA) with on or off options for the electron transport were performed. The relative error between the two optional simulation results can be given by Eq. (8).

$$\varepsilon = \frac{\mathrm{on} - \mathrm{off}}{\mathrm{on}} \times 100\% \quad (8)$$

The pencil-like MV x-ray beam is incident on the center of incident plane of a single block of $CdWO_4$

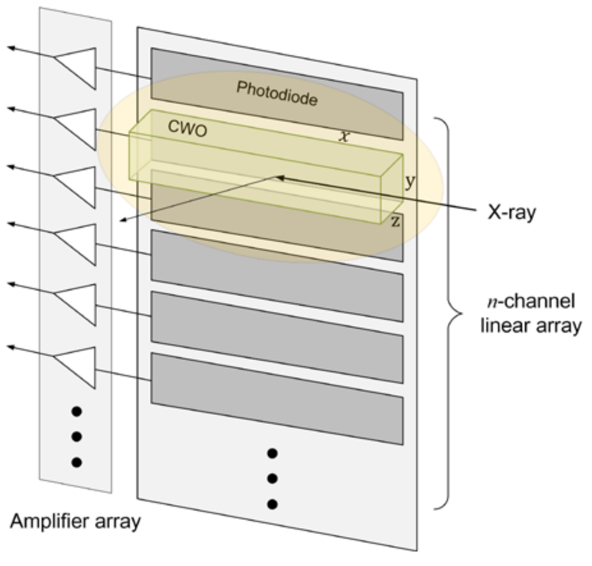

Figure 1. A linear $CdWO_4$ scintillation crystal and photodiode array used for the Monte Carlo simulations.

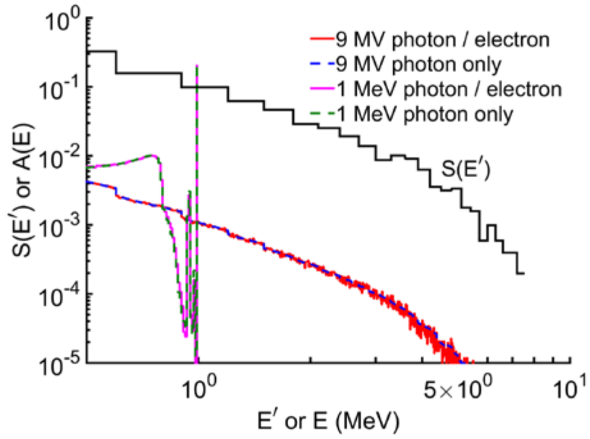

Figure 2. The absorbed energy distributions of the scintillation crystal obtained for Monte Carlo simulations.

scintillation crystal with dimensions of $x \times y \times z = x \times 4 \times 4$ mm^3 ($x = 10 \sim 50$ mm). The incident x-ray spectrum $S(E)$ is 9-MV spectrum or 1-MeV mono-energetic beam.

3. Preliminary Results

Fig. 2 shows the AED of the scintillation crystals obtained for MC simulations. While the AED obtained for monoenergetic beam clearly shows escape peaks due to Cd and W, that obtained for the MV spectrum shows no escape peaks. Electron interactions distort $A(E)$ in high energy bins.

For the quantitative signal-to-noise performance analysis, QE, Swank noise factor, DQE and relative error obtained for MC simulations are shown in Fig. 3.

As shown in Fig. 3(a) and (b), monoenergy analysis underestimates the QE performance and the degree of underestimation is increased with decreasing detector thickness. At the same time, monoenergy analysis overestimates the Swank noise factor by a factor of ~2.7 compared to the spectral analysis. And the consideration of the Swank factor of the incident spectrum can largely reduce the discrepancy between the two Swank analyses.

Fig. 3(c) shows that the increasing trend of DQE with increasing detector thickness is mainly governed by the QE. Monoenergy analysis largely overestimate the DQE performance because it ignores the spectral uncertainty in incident x-ray beam and this discrepancy can be reduced by considering the incident spectrum Swank factor.

In the Fig. 3(d), electron transport option would be negligible for the QE estimation. On the other hand, the consideration of the electron transport in determining $A(E)$ in high energy bins is important; hence the Swank noise factor.

4. Conclusions

For the given MV spectrum, the improvement of QE from a detector with a thickness of 10 mm to 30 mm is 27% whereas the improvement from 30 mm to 50 mm is only 7%. On the other hand, the Swank noise is almost independent of the detector thickness. Consequently, the improvement of DQE from a detector with a thickness of 10 mm to 30 mm is 46% whereas the improvement from 30 mm to 50 mm is only 11%.

In conclusion, the detector thickness of 30 mm would be the best for x-ray interaction-induced signal and noise performance as well as cost.

We also suggest that the monoenergy analysis considering the MV spectral Swank noise can provide DQE similar to that determined from the spectral analysis.

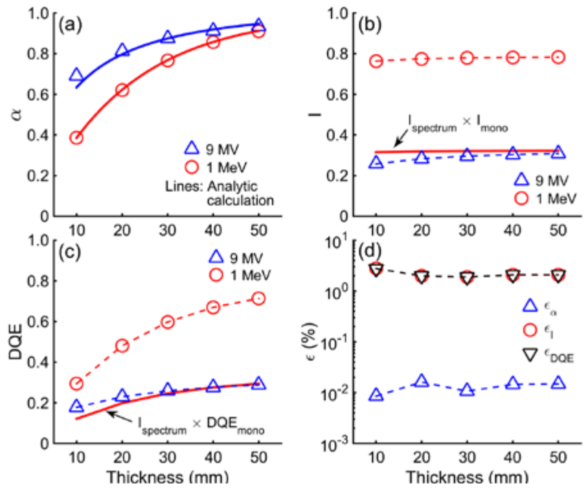

Figure 3. The quantitative signal-to-noise performances obtained for each simulations: (a) quantum efficiency, (b) Swank noise factor, (c) detective quantum efficiency, (d) relative error.

ACKNOWLEDGEMENT

This work was a part of the project titled 'Research on Fundamental Core Technology for Ubiquitous Shipping and Logistics,' funded by the Ministry of Oceans and Fisheries, Korea.

REFERENCES

[1] T.T. Monajemi, B.G. Fallone, and S. Rathee, "Thick, segmented CdWO4-photodiode detector for cone beam megavoltage CT: A Monte Carlo study of system design parameters," Med. Phys., Vol. 33, p. 4567, 2006.

[2] M. Kobayashi, M. Ishi, Y. Usuki, and H. Yahagi, "Cadmium tungstate scintillators with excellent radiation hardness and low background," Nucl. Instrum. Methods Phys. Res. A, Vol. 349, pp. 407-411, 1994.

[3] P. Kozma, R. Bajgar, and P. Kozma, Jr., "Radiation resistivity of large tungstate crystals," Radiat. Phys. Chem., Vol. 59, pp. 377-380, 2000

[4] D. R. Kinloch, W. Novak, P. Raby, and I. Toepke, "New developments in cadmium tungstate," IEEE Trans. Nucl. Sci., Vol. 41, pp. 752-754, 1994